JOURNAL OF BACTERIOLOGY, Aug. 1980, p. 1003-1018
0021-9193/80/08-1003/16$02.00/0

Vol. 143, No. 2

Transmission-Scanning Electron Microscopic Observations of Selected *Eikenella corrodens* Strains

ANN PROGULSKE AND S. C. HOLT*

Department of Microbiology, University of Massachusetts, Amherst, Massachusetts 01003

The morphology of *Eikenella corrodens* 333/54-55 (ATCC 23834) and two human periodontal lesion isolates, strains 470 and 373, was examined by transmission and scanning electron microscopy. All strains exhibited a cell envelope characteristic of gram-negative bacteria. Staining with ruthenium red and alcian blue revealed a loosely organized fibrous slime layer associated with the outer surface of the outer membrane. Slime "stabilization" was achieved by incubation of cells with antisera prepared against whole cells of the *Eikenella* strains. The stabilized slime appeared as a thick, electron-opaque layer juxtaposed to the outer membrane. Negative staining and heavy metal shadow-casting revealed an interwoven network of fibrils approximately 4 nm in diameter. These fibrils appeared to represent subunits of a larger fibril. Scanning electron microscopy after antibody slime stabilization confirmed the presence and location of the slime layer.

A variety of gram-positive and gram-negative procaryotic cells possess a layer external to, yet associated with, the outermost layer of the cell wall. This layer is referred to as the capsule, slime layer, ruthenium red-positive layer, and even glycocalyx. When organized into a regular morphologically structured component, it is usually referred to as a capsule; when loosely organized, or of variable consistency, it is most often designated a slime layer (38).

The production of a capsule or slime layer by procaryotic cells has multiple advantages for the bacterium: it can, for example, facilitate their attachment to both nonbiological and biological surfaces (6), function in virulence (27), and protect the cell from host defense mechanisms (32). This ability to attach or adhere to surfaces not only provides a potentially virulent bacterium with an intimate association which in many instances is a prerequisite for the establishment of disease (10, 31), but also affords the bacterium a mode of survival (see references 10, 11 for a discussion of bacterial adherence). The capsule also protects the bacterium from reaction of specific antibodies with bacterial-specific antigens located within the body of the cell (13). The capsule has also been shown to prevent the attachment of lipopolysaccharide-specific bacteriophages, as well as functioning as a site-specific structure for certain bacterial viruses (7).

Recently, several investigators have identified several bacterial types found in high numbers in both human (26, 34, 37, 39, 41) and animal (35; Kornman and Holt, unpublished data) periodontal pockets. *Eikenella corrodens* has been routinely recovered from deep gingival pockets of periodontitis patients (26, 37, 39). In addition, *Eikenella* strains have also been recovered from oral abscesses (19) and the upper respiratory tract (5, 14, 24). In fact, Badger and Peterson (Abstr. no. 962, J. Dent. Res. **57**:315, 1978) consider them to be a member of the normal oral flora. Interestingly, Badger and co-workers (1) were able to produce an experimental endocarditis in rabbits with *E. corrodens* strain 1073.

The following presentation describes the ultrastructural morphology of several strains of *E. corrodens*, one of sputum origin and two isolated from active cases of periodontitis. In all strains we report morphological characteristics which could function in bacterial-host interactions, which may not only affect the survival of the bacterium in its host, but so also function in the development of periodontal lesions.

MATERIALS AND METHODS

Organisms. The type strain, *E. corrodens* 333/54-55 (ATCC 23834), (14, 15, 17), was used, as well as fresh periodontal isolates designated *E. corrodens* 470 and 373. These latter strains were obtained from S. S. Socransky, Forsyth Dental Center, Boston, Mass.

Growth of organisms. Agar-grown cells were streaked to the surface of tryptose blood agar base (Difco Laboratories, Detroit, Mich.) supplemented with 5% (vol/vol) defibrinated sheep blood. The plates were incubated in Brewer jars (BBL Microbiology Laboratories, Cockeysville, Md.) under an atmosphere of 10% CO_2–90% air at 37°C for at least 4 days. For liquid growth, 3% (vol/vol) Todd-Hewitt broth (BBL Microbiology Systems) plus 0.5% (wt/vol) KNO_3, and 3 μg of hemin per ml were employed. Agar-grown cells

were used as inoculum for liquid cultivation. A loopful of cells was inoculated into tubes containing 10 ml of sterile broth and incubated for 48 h in Brewer jars under the CO_2–air atmosphere.

Preparation of antisera. Adult female New Zealand rabbits were used to prepare antisera against whole cells of *E. corrodens* strains 23834, 470, and 373. Four-day-old cells were removed from the agar surface and emulsified in 10 ml of Freund incomplete adjuvant. Five milliliters was injected both intramuscularly and subcutaneously. Antisera was raised over a 30-day period, at which time the rabbits were bled by cardiac puncture and the serum was separated from erythrocytes by low-speed centrifugation. All antisera were stored frozen (−20°C) until used. Before use, all antisera were filtered through 0.22-μm membrane filters (Millipore Corp., Bedford, Mass.) to remove large particles. The filtered antiserum was heat inactivated at 56°C for 30 min before use. Antibody titers were determined by macroscopic tube agglutination.

Light microscopy. Cells were scraped from the surface of blood agar plates, suspended in phosphate-buffered saline, and examined with a Zeiss GFL microscope (Carl Zeiss, New York, N.Y.) with oil immersion, phase-contrast optics.

TEM: glutaraldehyde-osmium fixation. For transmission electron microscopy (TEM), cells were fixed according to the method of Woo et al. (43). Cells were scraped from the surface of agar plates, fixed in 2% (vol/vol) glutaraldehyde in 0.1 M phosphate buffer, pH 7.2, at 4°C, washed with buffer, and post-fixed with 1% (wt/vol) OsO_4 in buffer overnight at 4°C.

Ruthenium red fixation and staining. *Eikenella* strains were processed with ruthenium red by the method of Woo et al. (43) as originally described by Luft (21). The bacteria were fixed in equal volumes of 3.6% (vol/vol) glutaraldehyde, 0.2 M cacodylate buffer and 0.22-μm-filtered ruthenium red (1,500 μl/liter in distilled water) for approximately 2 h. The cells were then washed with 0.2 M cacodylate buffer, and post-fixed in equal volumes of 4% (wt/vol) OsO_4, 0.2 M cacodylate buffer, and ruthenium red (1,500 μl/liter).

Alcian blue fixation and staining. Plate-grown cells were suspended in 0.5 ml of 0.1 M cacodylate buffer (pH 7.3), 0.5 ml of 3% (wt/vol) alcian blue 8GX (Taab Laboratories; Reading, England) in cacodylate buffer, and 0.5 ml of 3.6% (vol/vol) glutaraldehyde in cacodylate buffer and incubated at 4°C for 2 h (9, 40). The alcian blue-glutaraldehyde was removed, and the cells were washed at least four times with 0.1 M cacodylate buffer. All samples were post-fixed in 2% (wt/vol) OsO_4 containing 1% (wt/vol) alcian blue in 0.1 M cacodylate buffer overnight at 4°C.

All controls for ruthenium red and alcian blue consisted of 0.5 ml of cacodylate buffer substituted for the dye.

Treatment of bacteria with antisera. The *Eikenella* slime layer was stabilized by incubating cells at 37°C for 45 min with antiserum either undiluted or diluted in phosphate-buffered saline, pH 7.2. Unbound antibody was removed by washing the cells at least twice with 0.2 M cacodylate buffer, pH 7.2. Control preparations consisted of cells incubated in heat-inactivated normal rabbit serum and in phosphate-buffered saline alone. All samples were processed for electron microscopy as described for ruthenium red fixation and staining.

Dehydration and embedding. All samples were dehydrated through a graded ethanol series and embedded in Epon 812 (Polysciences, Warrington, Pa.).

Negative staining. Carbon-reinforced Formvar-coated grids were touched to the surface of *Eikenella* growth on agar plates. The cells were stained with a drop of either 3% (wt/vol) phosphotungstic acid, pH 7.3, or 2% (wt/vol) ammonium molybdate, pH 7.0, for at least 45 s, after which excess stain was removed with filter paper. The grids were air dried before viewing, which took place within 2 h of their preparation.

Platinum-carbon shadow-casting. Specimens were prepared as described for negative staining. The stage of a Balzers model 360M vacuum plant (Balzers High Vacuum Corp., Santa Ana, Calif.) was modified to accept electron microscope grids. The chamber was pumped into high vacuum (10^{-6} torr) and cooled with liquid nitrogen, and the specimens were shadowed at an angle of 20° with platinum-carbon evaporated from an Electron Beam Evaporation Gun EK552.

TEM observation. Thin sections were either stained with uranyl acetate and lead citrate (30) or examined unstained in a JEOL 100S electron microscope (Japanese Electronics Optics Laboratory, Peabody, Mass.), operating at 80 kV or a Philips EM 200 electron microscope (Philips Electronics, Einhoven, The Netherlands) operating at 60 kV.

SEM. Agar-grown cells were examined by scanning electron microscopy (SEM) directly on the agar surface. Cell-agar blocks (1 cm^2) were cut out with a clean razor blade and transferred to tubes of 2% (vol/vol) glutaraldehyde in 0.1 M phosphate buffer, pH 7.2. The samples were fixed for at least 7 days at 4°C. Liquid-grown cells were collected by passing a broth suspension through a 0.22-μm membrane (Nucleopore, Pleasanton, Calif.), slicing the membrane-impinged cells into 1-cm sections, and dehydrating and critical-point drying as described below.

Dehydration and critical-point drying. Fixed agar blocks and membrane filters were dehydrated in a graded acetone series before critical-point drying and Au-Pd coating (43). The dried cells were mounted on copper studs and stabilized with 10 to 20 nm of evaporated carbon. All samples for SEM observation were sputter coated with 20 to 40 nm of Au or Au-Pd from a Polaron E-5000 Sputter Coating Unit.

SEM observation. Specimens were examined with either a JEOL JSM 35 or a JSM 25 scanning electron microscope operating at 15 and 25 kV.

RESULTS

Titration of antisera. Agglutination titers of *E. corrodens* strains are reported in Table 1. High titers to each of the homologous antigens were obtained. With heterologous antisera, *E. corrodens* strains 23834 and 470 showed a close antigenic relatedness; however, a complete immunological identity was not detected between these strains. The lower titer of anti-470 serum

when reacted against whole cells of strain 23834 suggests different antigenic sites on the bacterial surfaces of strain 23834 or the uncovering of selective sites. There was less relatedness of these strains to *E. corrodens* strain 373.

Phase-contrast microscopy. Three-day-old, plate-grown *Eikenella* strains (Fig. 1) were uniformly rod-shaped, approximately 0.5 μm in diameter, and most often between 1.5 and 5 μm long, with an average diameter of 3.25 μm. Older cells (i.e., 7 and 11 days) tended to be shorter.

TEM: thin-sectioning. *E. corrodens* strains 23834, 470, and 373 (Fig. 2a, 3a and b) were morphologically identical to other gram-negative bacteria. The outer membrane was wrinkled, approximately 8 nm thick, and of unit construction. Directly beneath the outer membrane was the periplasmic space, which varied in density from transparent to granular. The thin, approximately 7-nm-diameter peptidoglycan occupied the periplasmic space and enclosed the unit cell or cytoplasmic membrane. The cytoplasmic region consisted of a central aggregated nucleoid surrounded by electron-opaque ribosomes. No cytoplasmic organelles or storage granules were visible. Characteristic of *E. corrodens* strains 23834 and 470 was the wrinkled, but smooth and "clean" outer surface of the outer membrane (Fig. 2a). Very few membrane vesicles (i.e., vesicle-lipopolysaccharide) or exopolymeric structures were found associated with the surface of the outer membrane. The outer membrane of *E. corrodens* strain 373, however, had associated with it a fibrillar material (Fig. 3a) or slime. We will use the term slime to denote the cell-associated exopolymeric material, the ruthenium red-, alcian blue-staining material, and the surface material observed by SEM and TEM of shadow-cast cells. In addition to covering the surface of the outer membrane, this slime was also free in the background.

TABLE 1. *Agglutination titers to homologous and heterologous E. corrodens strains 23834, 470, and 373 agglutinogens*

Antigen[b]	Tube agglutination titer[a] of antisera made against whole cells of:		
	23834	470	373
23834	1280	80	40
470	1280	1280	160
373	160	160	640

[a] Titers are expressed as the reciprocal of the highest dilution showing agglutination.

[b] Four-day old cells scraped from blood agar plates and suspended in phosphate-buffered saline.

To discern polyanionic molecules (i.e., polysaccharides), we employed ruthenium red and alcian blue stains with a high degree of specificity for polyanionic molecules (21, 33). When *E. corrodens* strain 23834 was fixed and stained with ruthenium red (Fig. 2c), thin ruthenium red-positive fibrils or strands of slime were apparent (compare with Fig. 2a). The ruthenium red-staining fibrils were associated with the surface of the outer membrane, as well as joining adjacent cells. *E. corrodens* strain 470 possessed large amounts of thin ruthenium red-positive fibrils (Fig. 2b), similar to strain 23834. In strain 470, however, the fibrils formed a net or webbed arrangement as they emerged from the surface of the outer membrane. It is not clear whether this webbed arrangement represents a preparative artifact (i.e., drying) or is a result of the contraction of the capsule or slime into fibrils during the staining process for TEM visualization. SEM revealed an almost continuous outer matrix material to these *E. corrodens* strains (see Fig. 9b).

Similar to ruthenium red, alcian blue stains

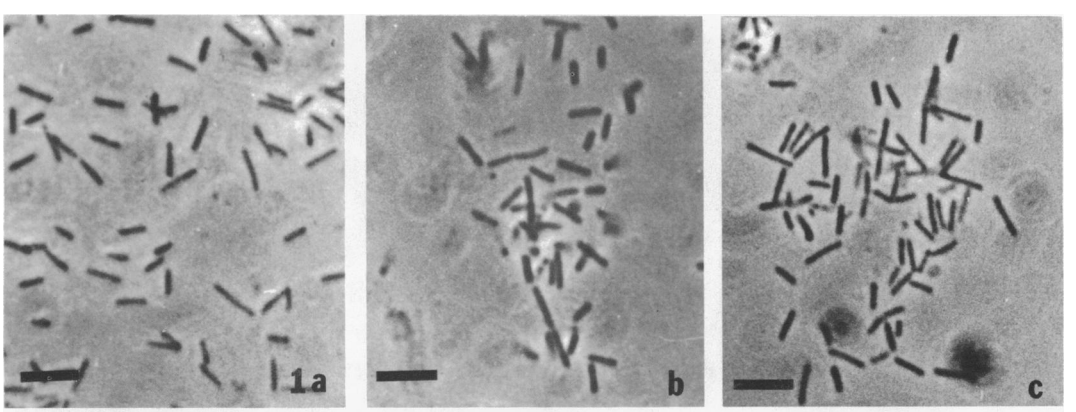

FIG. 1. *Phase-contrast photomicrographs of living cells of E. corrodens strains 470 (a), 23834 (b), and 373 (c). Plate grown, 3 days. Bar = 1 μm.*

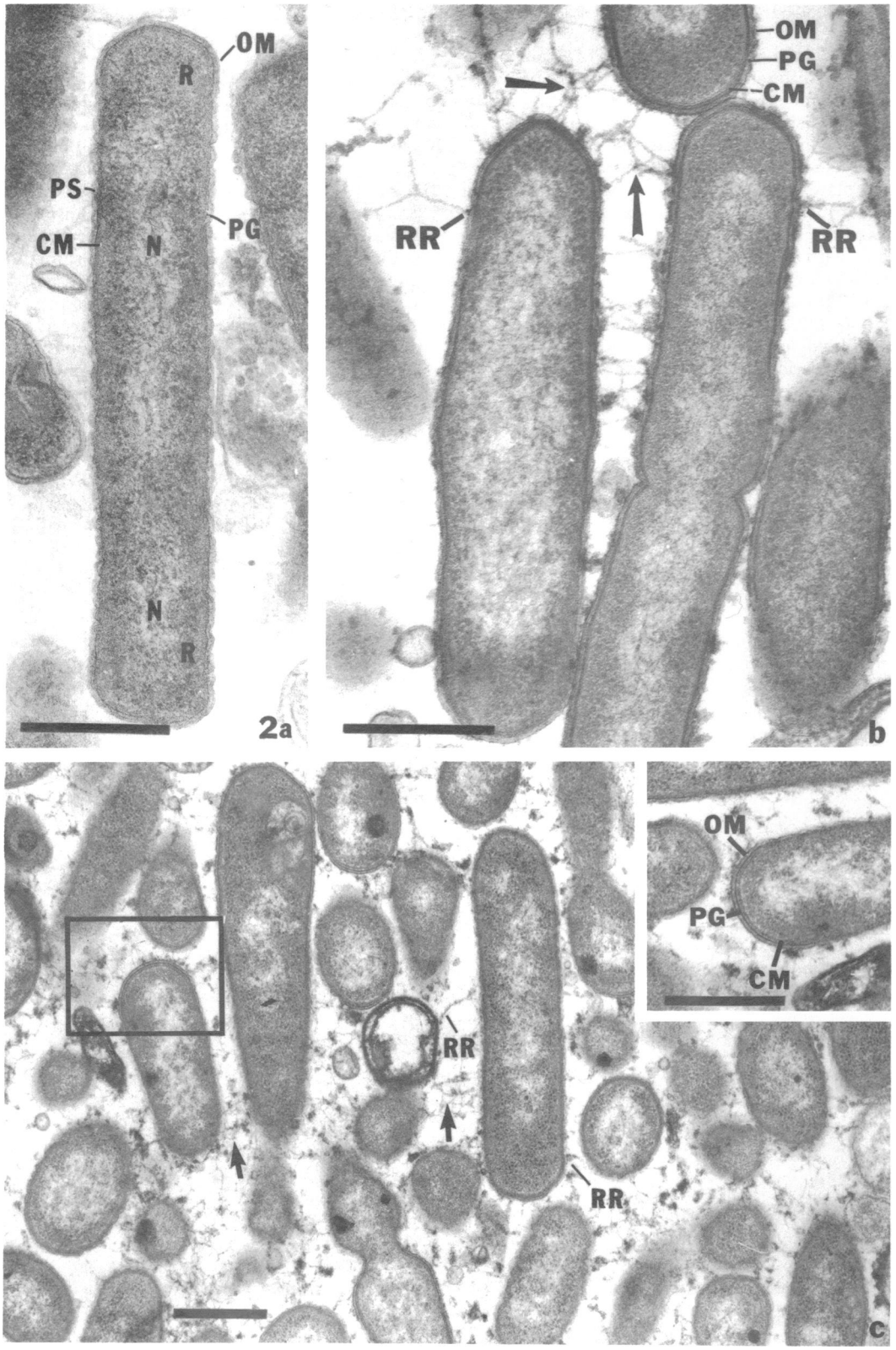
OM
R
PS
CM
N
PG
N
R
2a
OM
PG
CM
RR
RR
b
OM
PG
CM
RR
RR
c

acidic heteropolysaccharides, resulting in the deposition of electron-opaque insoluble complexes (21). Alcian blue staining of *E. corrodens* strain 373 revealed thick fibril aggregates, which emerged from, and were continuous with, the outer membrane (Fig. 3c). These alcian blue-staining fibrils took on a globular appearance, with some portions of them staining more intensely than other portions. Alcian blue also stained the surface of the outer membrane.

We employed the technique of antibody stabilization as described by Bayer and Thurow (2) and Mackie et al. (22) to obtain a clearer picture of the extent of the polyanionic slime layer in the *E. corrodens* strains. Specific antisera against homologous *E. corrodens* strains stabilized the exopolymer (Fig. 4) and prevented its collapse during preparative techniques as well as imparting electron opacity. In Fig. 4b and c *E. corrodens* strain 470 was reacted with its corresponding specific antiserum. The slime layer was stabilized into a compact and irregular electron-opaque layer. In Fig. 4b the antibody-stabilized slime surrounds the majority of cells, whereas in some cells it appears to have aggregated or localized into bundles of polymer.

Reaction of *E. corrodens* strain 470 with antiserum obtained against strain 23834 resulted in only a partial stabilization of the slime (Fig. 4d). In close juxtaposition to the surface of the outer membrane was the stabilized slime; however, thin delicate fibrils of unstabilized slime, extended away from the stabilized, organized slime layer. Even though the specific antibody-cell complex was washed at least twice with buffer, stabilized slime still remained in the background (Fig. 4b). The nonspecific sera appeared to react very weakly with the slime; however, it did not stabilize it on the surface of the cells outer membrane (compare with Fig. 4b and c).

Negative staining. Negatively stained *Eikenella* strains possessed numerous thin fibrils, each approximately 4 nm thick (Fig. 5b). Thick fibrils (Fig. 5a) ranged to 33 nm in diameter and most probably represent aggregates of the individual 4-nm fibrils. These fibrils were observed at all stages of *Eikenella* growth and appeared to emerge from all surfaces of the convoluted cell surface (Fig. 5c). Clearly in Fig. 5c, the thin fibrils are seen to comprise the thicker fibrils, and it appears that as they emerge from the cell surface, they unravel into the 4-nm structures.

Shadow-casting. By direct shadow-casting the *Eikenella* surface was convoluted (Fig. 6) typical of gram-negative bacteria similarly prepared. In Fig. 6a to c, *E. corrodens* 470 and 23834 were enrobed in a thin granular-textured slime. In addition, thin fibrils similar to those observed after negative-staining were also present. The fibrils were associated with the slime layer. Where the slime layer was either torn or stretched, the fibrils appeared to either be a part of it or associated with it. Whether the fibrils are distinct surface appendages, that is pili or fimbriae, or represent alterations of the slime layer is unknown. In Fig. 6c a layer of slime covers both the cells as well as occupying a major portion of the background. Also in Fig. 6c, fibers of various thicknesses are contained in, and form borders or edges of the slime layer. *E. corrodens* strain 373 (Fig. 6d) possessed a surface slime which was more aggregated and globular in appearance. In addition, strain 373 appeared to possess more fibrils than strains 470 and 23834. Note in Fig. 6d that, in addition to being aggregated, fibrils also were formed into an intertwined web rather than existing as individual structures.

SEM. Figure 7 describes the morphological events observed after critical-point drying and SEM of agar-grown *E. corrodens* strain 23834 as a function of cell age. After 48 h of incubation, (Fig. 7a and b), the cells were relatively smooth, with only a slight pebbled surface texture. Short, thin fibrils joined adjacent cells. These fibrils emerged from several points along the cell surface, and were probably similar to, if not identical with the ruthenium red- and alcian blue-staining fibrils (Fig. 2b, c, and 3c). Continued incubation of *E. corrodens* 23834 for 7 (Fig. 7c) and 11 days (Fig. 7d) resulted in the formation of a thick, amorphous matrix or slime which completely enrobed the cells. The thin fibrils which connected adjacent cells at 48 h (Fig. 7b), were now thick and webbed and traversed great distances. Characteristic of the cells at these latter stages of growth was the change in cell morphology from a rod shape to a coccobacillary

FIG. 2. *Thin-sections of chemically fixed cells of E. corrodens strains 23834 (a) prepared by glutaraldehyde-osmium fixation and stained with uranyl acetate and lead citrate. The outer membrane (OM) is wrinkled and free of adhering extracellular polymer. The peptidoglycan (PG) occupies the periplasmic space (PS) external to the unit cell membrane (CM). The cytoplasmic region consists of a central nucleoid (N) surrounded by electron-opaque ribosome particles (R). Cells of strains 470 (b) and 23834 (c) fixed and stained with ruthenium red-OsO_4. Ruthenium red-positive fibrils (RR) cover the surface of the outer membrane and join adjacent cells (arrows). The various cell envelope layers are seen more clearly in the inset in (c) a higher magnification of the enclosed area. Bar = 0.5 μm.*

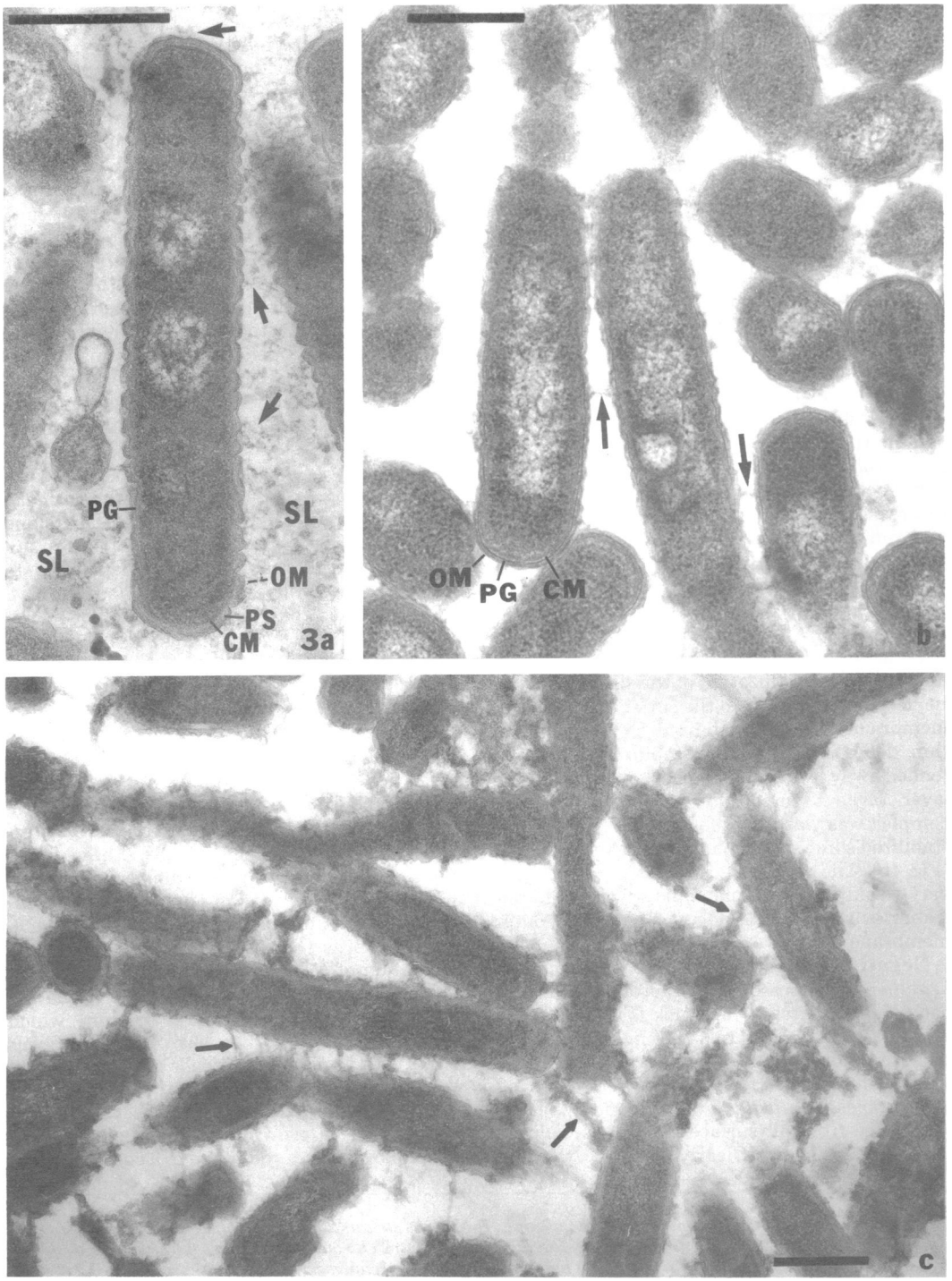

FIG. 3. *Thin sections of E. corrodens strain 373 fixed with glutaraldehyde-osmium tetroxide and stained with lead citrate and uranyl acetate (a). Large amounts of extracellular slime (SL) both free in the section background and associated with the surface of the outer membrane (arrows) is apparent. The periplasmic space (PS) encloses the peptidoglycan (PG). Alcian blue staining of strain 373 (c) reveals thick fibrils emerging from the surface of the outer membrane (arrows). The alcian blue control (b) lacks the thick fibrils; several thin fibrils do occur (arrows). Bar = 0.5 μm.*

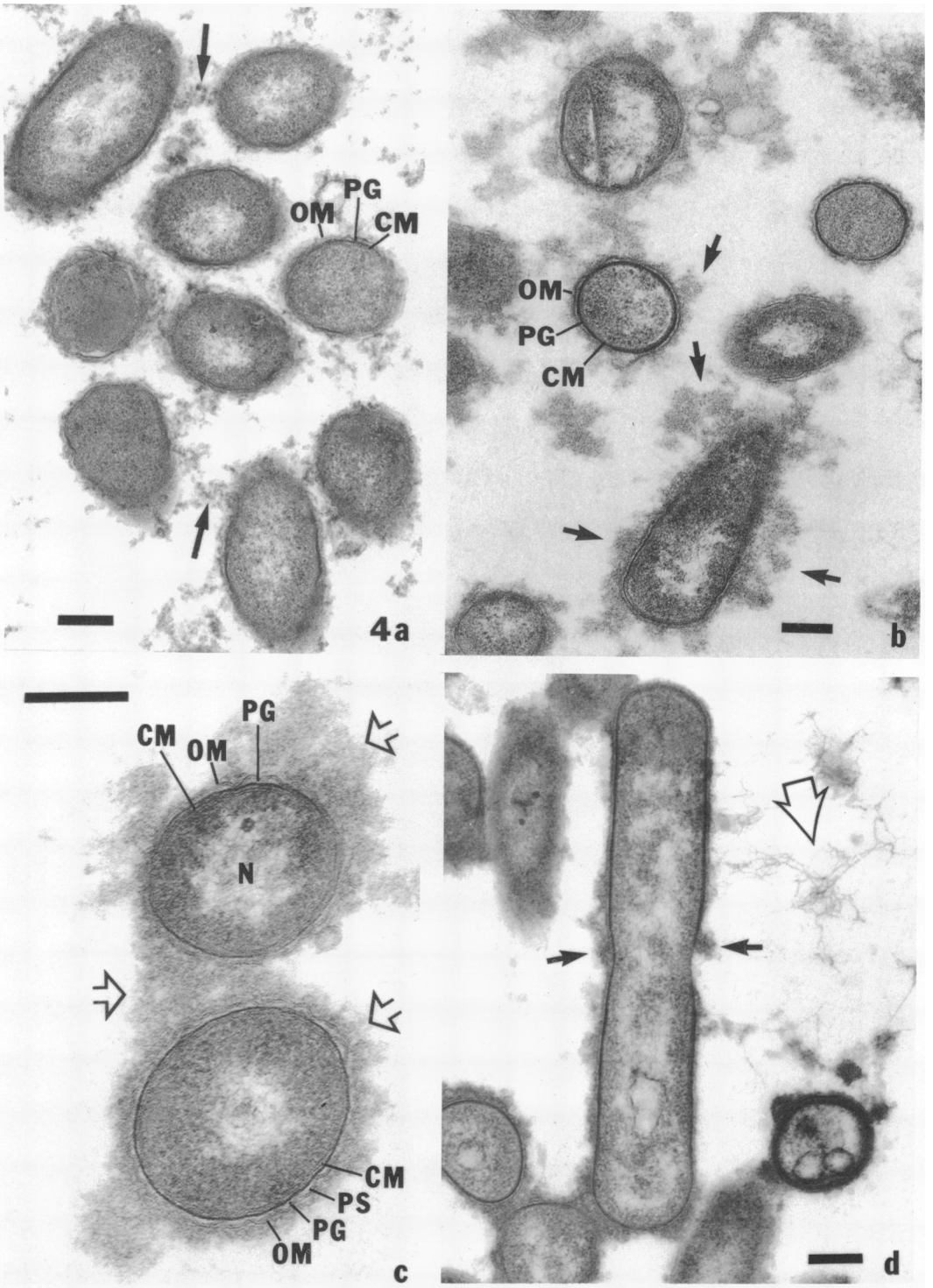

FIG. 4. *Thin sections of E. corrodens strain 470 after reaction with normal heated rabbit serum (a), homologous antiserum (b, c), and heterologous antiserum prepared against strain 23834 (d). In (a), there is only minor slime stabilization (arrows). Incubation of strain 470 with homologous antiserum (b, c) results in slime stabilization into a thick, electron-opaque layer (arrows). Partial stabilization of the slime layer in E. corrodens strain 470, when reacted with heterologous antiserum (to E. corrodens strain 23834) is seen in (d). The slime layer is stabilized in small patches (arrows), and thin fibrils (large arrow) extend away from the outer membrane surface. Bar = 250 nm.*

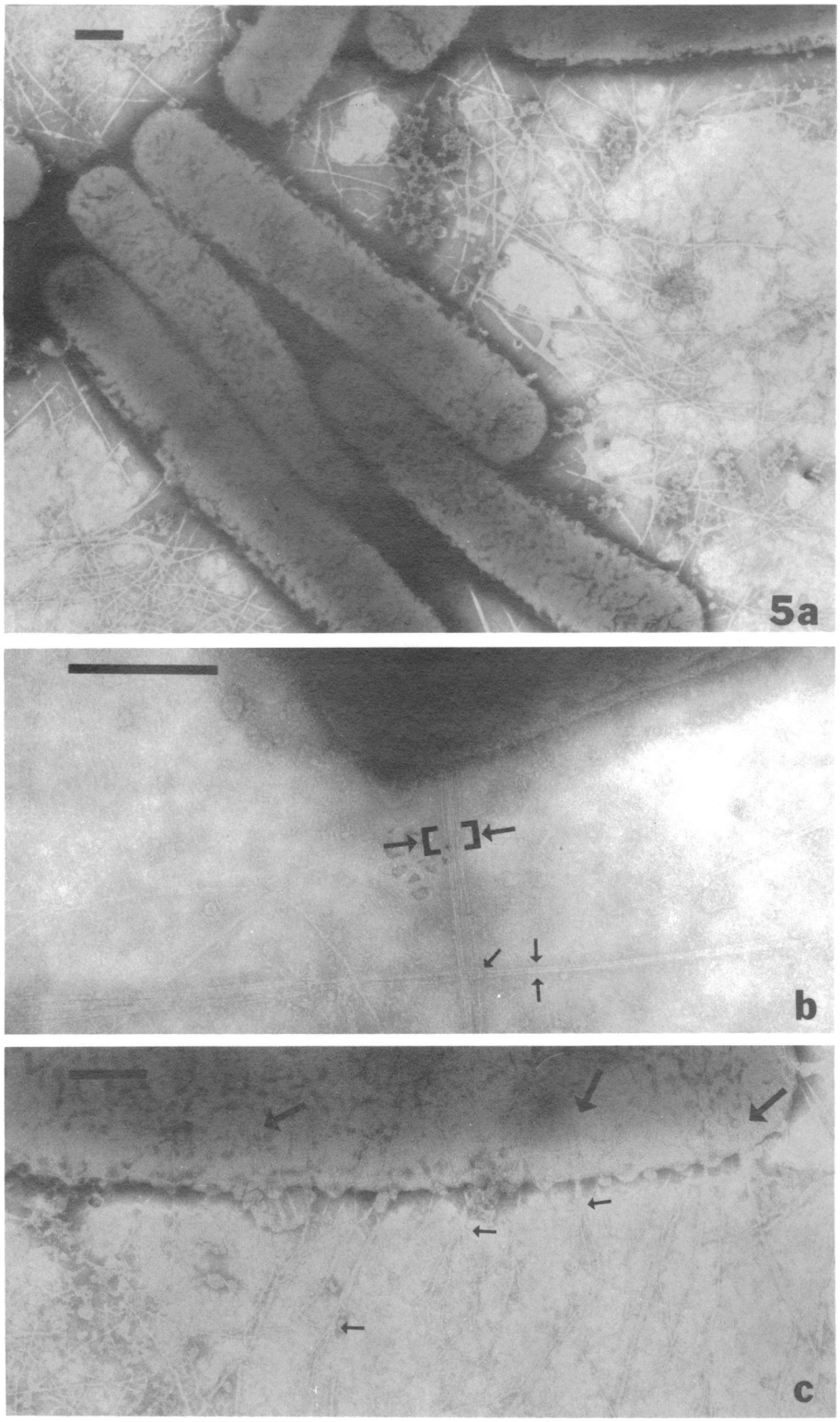

FIG. 5. *Negatively stained cells of E. corrodens strain 373. Numerous 33-nm-thick fibrils emerge from all cell surfaces (a), more clearly seen in (c). In (b), the fibrils are composed of a large fibril (large arrows) which has unravelled into thin 4-nm strands (small arrows). In (c), the 33-nm fibrils occur along the entire surface of the cell (large arrows). As the fibrils leave the cell proper, they unravel into the 4-nm-diameter structures (small arrows). Bar = 250 nm. Negative stain, 1% NH_4MoO_4, pH 7.0.*

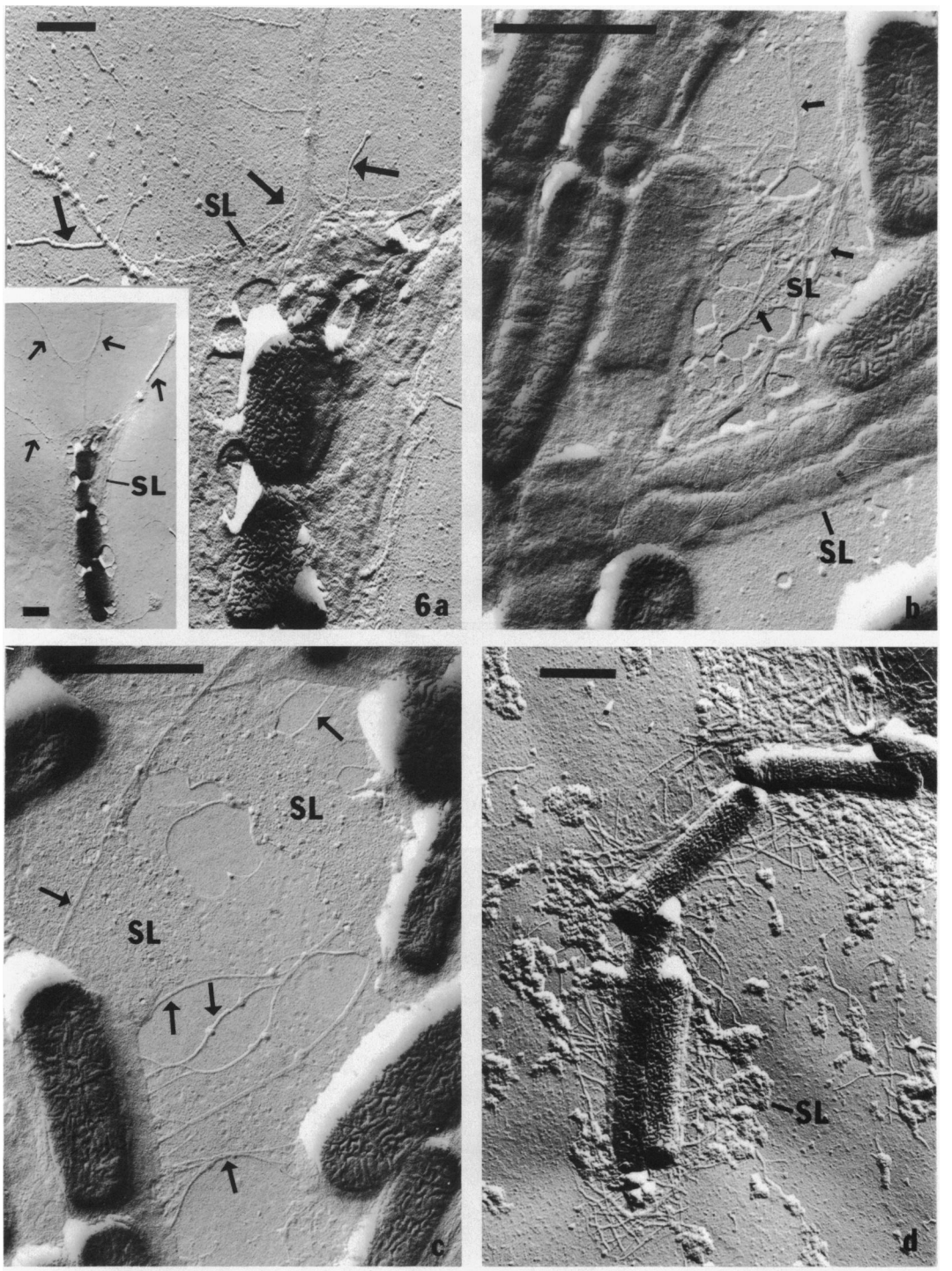

FIG. 6. *Shadow-cast E. corrodens strains 470 (a), 23834 (b, c), and 373 (d). The granular textured slime layer (SL) covers the cells in a mesh (a, inset). At higher magnification the slime layer has associated with it, long, thin fibrillar extensions (arrows), clearly a part of the slime layer (a–c, arrows). In (c) several thick fibrils emerge from the surface of the slime. A more aggregated and globular slime and intertwined fibrillar web is seen with cells of E. corrodens strain 373 (d). Shadow angle 20°; carbon-platinum alloy. Bar = 1 μm.*

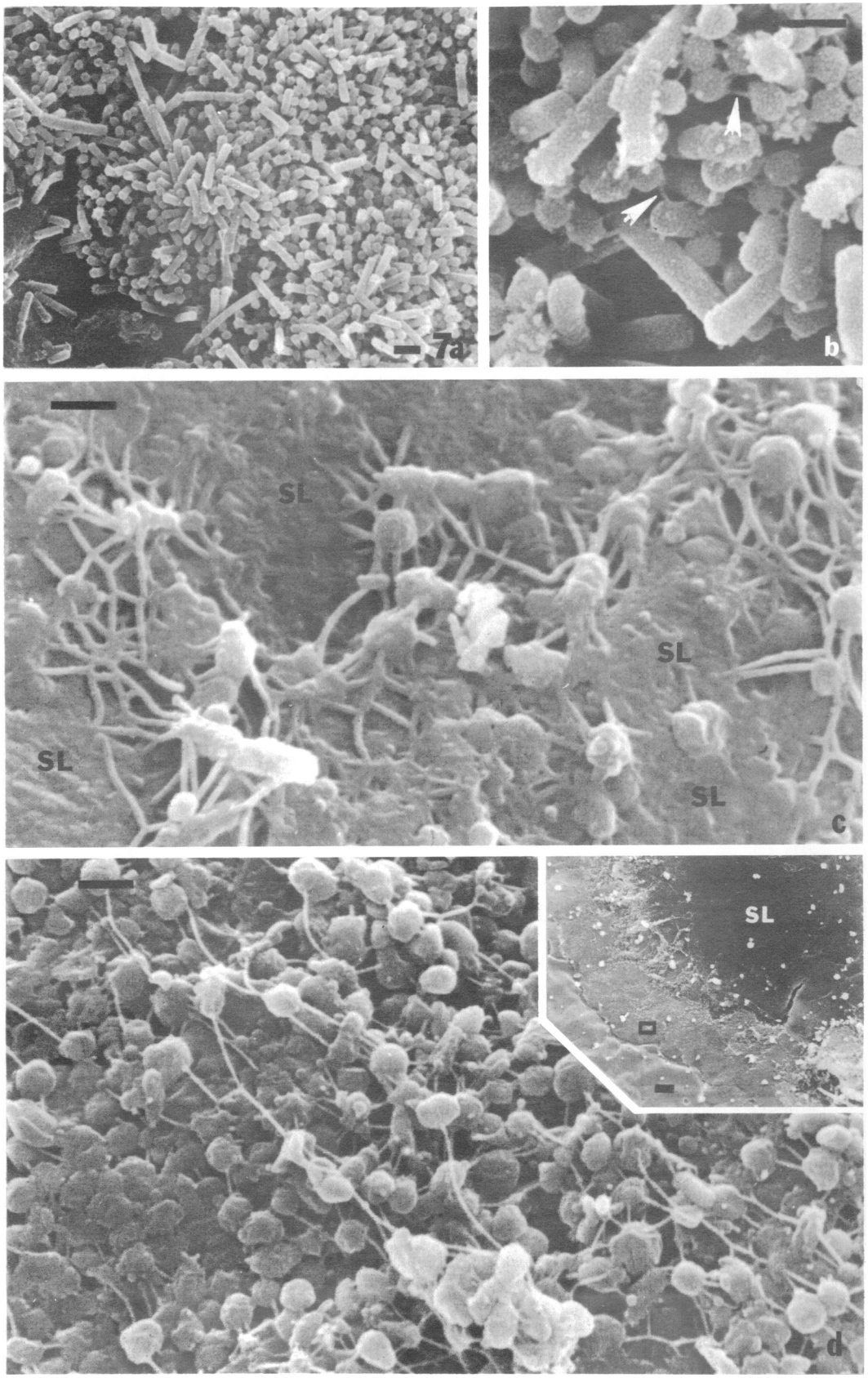
7a
b
SL
SL
SL
SL
c
SL
d

morphology. At 11 days the colony centers were covered by an amorphous matrix material (Fig. 6d inset), whereas cells at the colony periphery were interconnected by thick fibrils (Fig. 7d). Although we could recover viable cells by solid-liquid or solid-solid transfer, the percent cell viability at 11 days was low.

E. corrodens strain 373 did not form the long, thick fibrils characteristic of strain 23834 and 470 (see Fig. 7c and 8c). Instead, this strain was covered with a globular arrangement of particles, most probably representative of torn or contracted outer covering or slime layer (Fig. 8b). In some sections of a developing colony of *Eikenella* strain 470, large masses of intertwined fibrils (Fig. 8c and d) were apparent. In Fig. 8c, the extensive slime layer produced by *E. corrodens* strain 470 takes on a webbed appearance, and in Fig. 8d large amounts of cell-free slime are seen.

Slime was also observed in liquid-grown *E. corrodens* strains. For example, after 48 h of incubation in broth, strain 23834 (Fig. 8a), although not covered with the thick slime characteristic of plate-grown cells, was connected by numerous thin fibrils (characteristic of 48-h plate-grown cells, Fig. 7b). The cell-cell association through surface fibrils were clearly evident, as were surface particles or knobs which most probably are representative of collapsed or contracted slime.

The antibody-slime stabilization procedure was also employed for SEM. By reacting whole cells with antiserum before the preparative techniques for SEM, the slime layer was stabilized against the possible adverse affects of solvent dehydration and drying. When *E. corrodens* 23834 was reacted with homologous antiserum, critical-point dried, and observed by SEM (Fig. 9b), the cells were covered with a thick globular matrix of slime. The thick fibrils seen in Fig. 7c were no longer visible; the specific antiserum had stabilized the slime and distributed it over the cell surface in a globular arrangement. Reaction of *E. corrodens* strain 470 with 23834 antiserum (Fig. 9c) resulted in only a partial stabilization of slime as both a globular matrix and fibrils. Cells treated with preimmune heat-inactivated rabbit serum (i.e., control, Fig. 9a) showed no slime stabilization.

DISCUSSION

Luft (21) employed ruthenium red as a stain for the localization of acid mucosubstances in the ultrastructural analysis of animal tissues. Pate and Ordal (29) and Springer and Roth (36) extended Luft's technique to bacteria for the localization of acidic polyanionic compounds (i.e., mucopolysaccharides) on bacterial cell surfaces. Most recently, extracellular materials associated with the surface of the outer membrane of several gram-negative bacteria isolated from periodontal pockets have been shown to be ruthenium red positive. Holt et al. (16) observed a ruthenium red-positive "fuzz" on the outer membrane surface of several *Capnocytophaga* strains, and Woo and co-workers (43) demonstrated the existence of a ruthenium red-positive layer of variable thickness and construction associated with the surface of various oral and nonoral isolates of the genus *Bacteroides*. Similar ruthenium red-positive layers have been observed on the surface of several strains of *Actinobacillus actinomycetemcomitans* (S. C. Holt, A. C. R. Tanner, and S. S. Socransky, submitted for publication).

Although alcian blue has been employed for the histological localization and identification of polyanionic polymers (9, 40), there have been few reports (8) of its use with procaryotic cells. Beveridge (personal communication) has attempted to use the stain with several bacteria, but has not met with consistent success. With the *Eikenella* strains which we have examined, alcian blue stained the slime with a much finer consistency when compared with ruthenium red-stained cells. Interestingly, when one *Eikenella* strain stained with ruthenium red, it stained poorly with alcian blue. Thus, strain 23834, which was ruthenium red positive, was alcian blue negative, whereas strain 373, which was alcian blue positive, was ruthenium red negative. Whether this difference in staining quality reflects stain-exopolymer interactions characteristic of physical or chemical differences (i.e., ruthenium red interacting chemically or physically with different chemical groups in the polymer) is unknown.

The relatively high degree of hydration of bacterial slimes and capsules (with reports of

FIG. 7. *SEM of plate-grown E. corrodens strain 23834. Cells grown for 2 days (a, b) have a slightly rough-textured surface. Numerous thin fibers (arrows, b) connect adjacent cells. By 7 days of incubation (c), colonies are covered with a thick amorphous matrix (slime? SL). Numerous thick fibers are also present. At 11 days of incubation (d), colony centers are almost completely covered by the slime (SL) (d, inset). Panel d is a higher magnification of the outlined area in d, inset. Cells at the colony periphery exhibit a coccobacillary morphology and are interconnected by long, thick filaments. Bar = 1 μm; inset bar = 10 μm.*

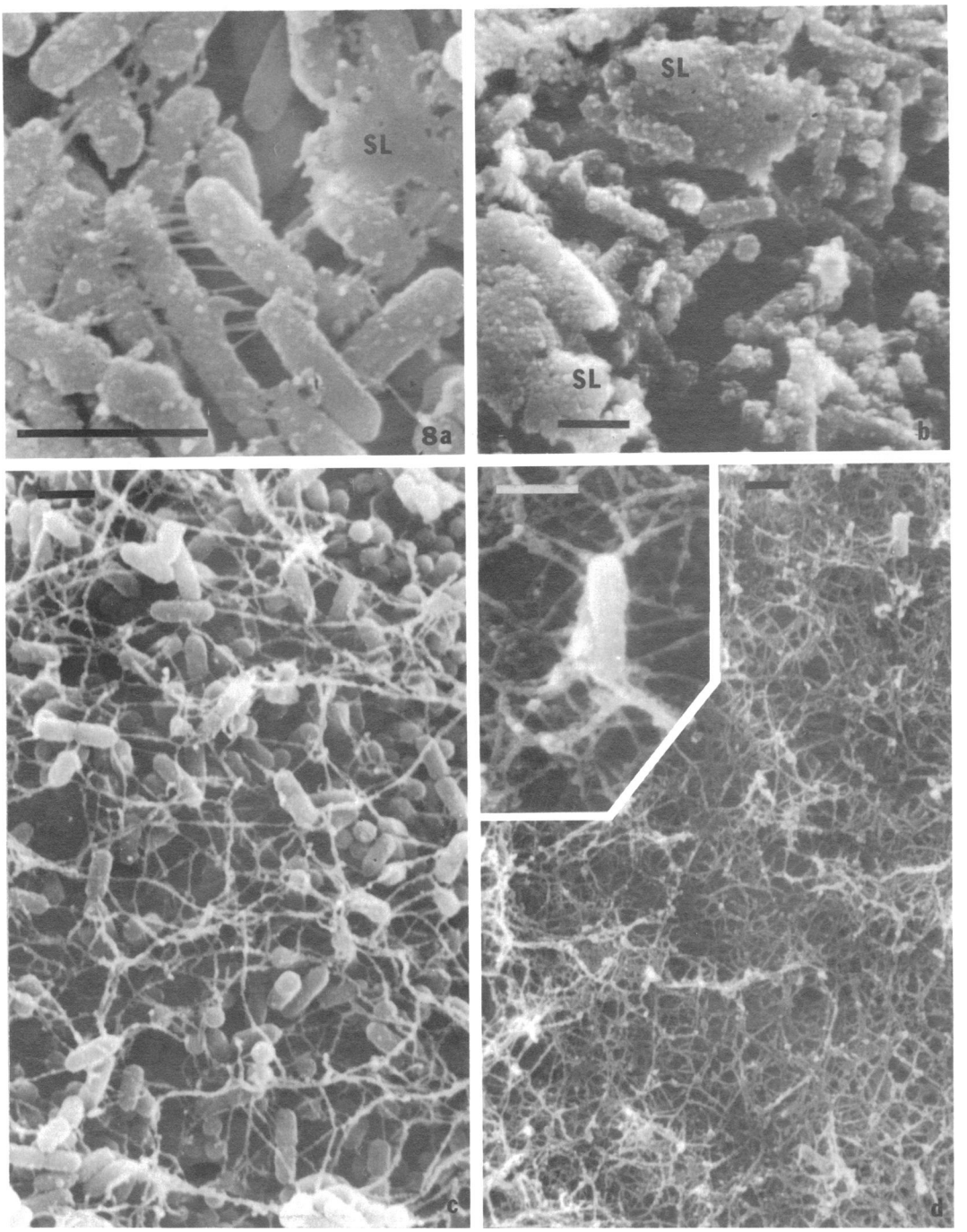

FIG. 8. *SEM of 48-h liquid-grown E. corrodens strain 23834 (a) and 4-day plate-grown cells of strain 373 (b) and 470 (c, d). Numerous particles and surface fibers cover the cell surfaces. Slime fragments (SL) are seen in (a, b). These strains produce large amounts of slime which appear as an intertwined, webbed matrix (c, d). In panel d a large mass of slime occurs without associated bacteria. The inset in panel d reveals one cell still intimately associated with the slime matrix. Bar = 1 μm.*

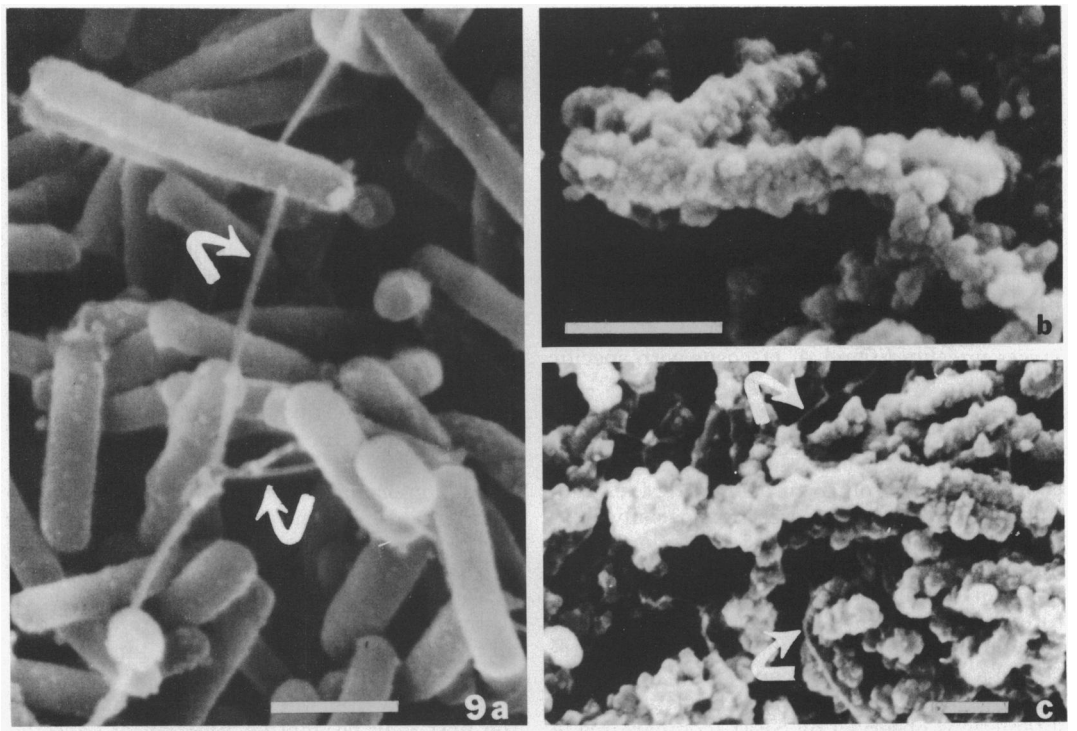

FIG. 9. *SEM of E. corrodens strain 23834 after reaction with normal heated rabbit serum (a) and homologous antiserum (b) and after reaction of strain 470 with antiserum against strain 23834 (c). Control cells (a) are relatively smooth, with some exhibiting granular-textured, particule-covered surfaces. Thick fibers connect neighboring cells (arrows). In the presence of homologous antiserum (b), the cell surface is covered by a thick globular matrix, and no fibers are seen. In the presence of anti-23834 serum, strain 470 (c), demonstrated only a partial stabilization of the slime as evidenced by the presence of fibers (arrows). Bar = 1 μm.*

>95% hydration of acid mucopolysaccharides for *Klebsiella aerogenes* capsules, 38) makes it almost impossible to fix or stabilize the polymers in a fashion characteristic of structures which most probably occur in the native state. Thus, fixatives such as glutaraldehyde and osmium tetroxide, while fixing proteins and lipids, do not fix the acidic mucopolymers in a physical or chemical state that permits their visualization with stains usually employed in classical TEM (i.e., lead, uranyl salts). Ruthenium red and alcian blue also do not stabilize these highly hydrated molecules, but interact in such a way to permit their visualization as, in most instances, stranded or fibrillar networks. These stranded fibrils are most probably not representative of the native configuration of the exopolymer (i.e., slime), since these fibrils are absent after immunocoating of cells prepared for SEM or TEM observation (compare Fig. 9b and c with Fig. 8a and c and Fig. 4b and c with Fig. 2b and c). Bayer and Thurow (2) reported, for example, the irreversible collapse of *Escherichia coli* capsules when exposed to at least 50% acetone or alcohol during the dehydration procedure for electron microscopy. By pretreatment of the cells with increasing concentrations of capsule-specific immunoglobulin G, they were able to stabilize the polysaccharide capsule into a uniform dense coat of smooth texture closely resembling the capsule structure seen with freeze-etched cells in which no chemical dehydration occurs. Thus, the stabilized capsule according to Bayer and Thurow (2) was probably not due to immunoglobulin molecules aggregated at the cell surface, but to a chemical stabilization. Bayer and Thurow (2) further proposed that capsular stabilization in their *E. coli* strain was the result of cross-linking of the capsular polysaccharide subunits with the immunoglobulins producing a more rigid structure. Mackie et al. (22) employed specific immunoglobulins to stabilize and enhance the ruthenium red positive streptococcal glycocalyx. The small, compact or aggregated capsules seen with standard ruthenium red-stained streptococci became stabilized

into more extensive networks with the addition of specific antisera. These investigators also supported the proposal by Bayer and Thurow (2) that the immunoglobulin-stabilized capsules closely resemble the undisturbed capsular structure, since critical point-dried cells possessed capsules similar to that of antibody-treated and thin-sectioned cells. *E. corrodens* prepared by shadow-cast techniques (Fig. 6) demonstrated large sheets of slime, also supporting immunoglobulin stabilization of capsular/slime structure. Lai and Listgarten (20) were also successful in "immunocoating" the capsules of *Actinomyces naeslundii* and *A. viscosus* with specific antisera.

Even though critical-point drying results in minimal dehydration stress, it also is plagued with surface tension forces which could pull, contract, and distort a surface matrix (i.e., capsule or slime). These stresses are especially prevalent during organic solvent dehydration. Thus, fibers and filaments seen in SEM preparations may not be representative of the actual structures, especially since our TEM observations of specific antibody-*Eikenella* interactions revealed a more continuous and globular network similar if not identical to specific antibody-cell interactions observed by SEM (compare Fig. 4 with Fig. 9). Most likely antibody stabilization minimizes artifacts of organic solvent dehydration, and critical-point drying–SEM of specific antibody-reacted cells is most representative of the slime in its most undisturbed state.

The macroscopic tube agglutinations, staining characteristics, and differences in heterologous antibody stabilization of exopolymer of *E. corrodens* 373, in contrast to those of strains 23834 and 470, indicate that the latter exopolymers are closely related biochemically, whereas the exopolymer of strain 373 is different. These differences could be reflected in protein concentration or degree of exopolymer hydration or both, since the exopolymer of strain 373 was "visible" without specific stains.

We are still unclear as to whether the *E. corrodens* strains examined produce pili, or whether the fibrils observed by the various morphological techniques employed are a product of a larger surface structure, such as the slime layer. Care must be exercised in the interpretation of shadow-cast and negative-stained preparations, because the cells are subjected to numerous surface stresses which could produce structural artifacts. In addition, the slime layer in *E. corrodens* appears to be both unstructured and loosely organized around the cell, lending itself to possible reorganization into several morphological configurations during the preparative techniques for electron microscopy. Our observation that the fibrils are in close association with the slime layer (see for example Fig. 6) and in some cases appear to be extensions of it leads to a major uncertainty as to their exact nature. In spite of their thickness (4 nm) and morphology, which is consistent with that reported for pili (4, 28), other investigators (18) have observed in anaerobic corroding bacilli (*Bacteroides corrodens*) polar processes which they equate with pili. Similarly, when *Sporocytophaga myxococcoides* and *Cytophaga hutchinsonii* were examined after negative-staining, an interwoven extracellular fibrillar matrix (elementary fibrils) was observed, the fibrils of which were approximately 3 nm in diameter (25). Morphologically, these extracellular fibrils were similar to those observed by us in *Eikenella*.

The importance of capsulated gram-negative microorganisms in the pathogenesis of abscesses was convincingly shown in an interesting series of experiments by Onderdonk et al. (27). These investigators showed that only capsulated strains of *Bacteroides fragilis* were capable of abscess formation when inoculated in pure culture into the rat pelvic region.

Protection from the immune mechanisms of the host may be another function of bacterial exopolymers. Slime from a strain of *Pseudomonas aeruginosa* isolated from a cystic fibrosis patient reportedly had antiphagocytic properties not only for the pseudomonad, but also for *E. coli* and *Staphylococcus aureus* (32). Wilkinson and co-workers (42) reported that the *S. aureus* capsule interfered with opsonization by normal human serum, preventing phagocytosis by polymorphonuclear leukocytes. Similar results were reported by Maheswaran and Thies (23) with *Pasteurella multocida*. The interference in phagocytic activity with *P. multocida* was attributed to the presence of hyaluronic acid in the capsule.

Bacterial slimes and capsules have also been observed to interfere with the humoral defense mechanism of the host. Glynn and Howard (13) found, for example, that there was a direct correlation between the quantity of *E. coli* K antigens (surface-associated polysaccharide-containing compounds) and complement insensitivity. They observed that complement resistance was directly proportional to the amount of K antigen present on the cell surface, and a decreased binding of immunoglobulin G and immunoglobulin M antibodies was a direct function of the cells' K-antigen content.

Possible biological activities of a partially purified slime extract and a lipopolysaccharide fraction of *E. corrodens* strains CS10 A and CS10 B have been investigated by Behling and co-work-

ers (3). The *E. corrodens* CS10 A lipopolysaccharide showed typical endotoxic activities; however, the slime extract exhibited little endotoxic activity. It did appear, however, to have a definite immunosuppressive affect.

Given few indications of bacterial infiltration into gingival tissues in periodontitis (12), bacterial components or the reaction of the host to these components are prime mechanisms of the tissue destruction observed in periodontal diseases. The slime of *E. corrodens* and other bacteria could afford many advantages to the microorganism and may be likely candidates as essential components in the pathogenesis of noninvasive or inflammatory diseases in general.

ACKNOWLEDGMENT

This investigation was supported by Public Health Service grant DE-05123 from the National Institute of Dental Research. The JEOL JSM35 scanning electron microscope was provided by National Science Foundation grant BMS 75-02883, and the JEOL 100S transmission electron microscope by National Science Foundation grant PEM 78-05656.

We thank Erika Musante for her continued interest and participation in all of this work and T. Beveridge for supplying the alcian blue.

LITERATURE CITED

1. **Badger, S. J., T. Butler, C. K. Kim, and K. H. Johnston.** 1979. Experimental *Eikenella corrodens* endocarditis in rabbits. Infect. Immun. **23**:751-757.
2. **Bayer, M., and M. Thurow.** 1977. Polysaccharide capsule of *Escherichia coli*: microscopic study of its size, structure, and sites of synthesis. J. Bacteriol. **130**:911-936.
3. **Behling, U. H., P. Pham, and A. Nowotny.** 1979. Biological activity of the slime and endotoxin of the periodontopathic organism *Eikenella corrodens*. Infect. Immun. **26**:580-584.
4. **Brinton, C. C., Jr.** 1965. The structure, function, synthesis and genetic control of bacterial pili and a molecular model for DNA and RNA transport in Gram negative bacteria. Trans. N. Y. Acad. Sci. Ser. II **27**:1003-1054.
5. **Brooks, G. F., J. M. O'Donoghue, J. P. Rissing, K. Soapes, and J. W. Smith.** 1974. *Eikenella corrodens*, a recently recognized pathogen: infections in medical-surgical patients and in association with methylphenidate abuse. Medicine **53**:325-342.
6. **Costerton, J. W., G. G. Geesey, and K.-J. Cheng.** 1978. How bacteria stick. Sci. Am. **238**:86-95.
7. **Fehmel, F., U. Feige, N. Niemann, and S. Stirm.** 1975. *Escherichia coli* capsule bacteriophages. VII. Bacteriophage 29-host capsular polysaccharide interactions. J. Virol. **16**:591-601.
8. **Fletcher, M., and G. D. Floodgate.** 1973. An electron-microscopic demonstration of an acidic polysaccharide involved in the adhesion of a marine bacterium to solid surfaces. J. Gen. Microbiol. **74**:325-334.
9. **Geyer, G., U. Helmke, and A. Christner.** 1971. Ultrahistochemical demonstration of alcian blue stained mucosubstances by the sulfide-silver reaction. Acta Histochem. **40**:80-85.
10. **Gibbons, R. J.** 1977. Adherence of bacteria to host tissue, p. 395-406. *In* D. Schlessinger (ed.), Microbiology-1977. American Society for Microbiology, Washington, D.C.
11. **Gibbons, R. J., and J. van Houte.** 1975. Bacterial adherence in oral microbial ecology. Annu. Rev. Microbiol. **29**:19-44.
12. **Gibson, W. A., and I. C. Shannon.** 1964. Microorganisms in human gingival tissues. Periodontol. **2**:119-121.
13. **Glynn, A. A., and C. J. Howard.** 1970. The sensitivity to complement of strains of *Escherichia coli* related to their K antigens. J. Immunol. **18**:331-346.
14. **Henriksen, S. D.** 1969. Corroding bacteria from the respiratory tract. 2 *Bacteroides corrodens*. Acta Pathol. Microbiol. Scand. **75**:91-96.
15. **Henriksen, S. D.** 1969. Designation of the type strain of *Bacteroides corrodens* Eiken 1958. Int. J. Syst. Bacteriol. **19**:165-166.
16. **Holt, S. C., E. R. Leadbetter, and S. S. Socransky.** 1979. *Capnocytophaga:* a new genus of Gram-negative gliding bacteria. II. Morphology and ultrastructure. Arch. Microbiol. **122**:17-27.
17. **Jackson, F. L., and Y. E. Goodman.** 1972. Transfer of the facultatively anaerobic organism *Bacteroides corrodens* Eiken to a new genus, *Eikenella*. Int. J. Syst. Bacteriol. **22**:73-77.
18. **Jackson, F. L., Y. E. Goodman, F. R. Bel, P. Wong, and R. L. S. Whitehouse.** 1971. Taxonomic status of facultative and strictly anaerobic "corroding bacilli" that have been classified as *Bacteroides corrodens*. J. Med. Microbiol. **4**:171-183.
19. **Jones, J. L., and D. A. Romig.** 1979. *Eikenella corrodens:* a pathogen in head and neck infections. Oral Surg. **48**:501-505.
20. **Lai, C.-H., and M. A. Listgarten.** 1979. Immune labelling of certain strains of *Actinomyces naeslundii* and *Actinomyces viscosus* by fluorescence and electron microscopy. Infect. Immun. **25**:1016-1028.
21. **Luft, J. H.** 1971. Ruthenium red and violet. I. Chemistry, purification, methods of use for electron microscopy and mechanism of action. Anat. Rec. **171**:347-368.
22. **Mackie, E. B., K. N. Brown, J. Lam, and J. W. Costerton.** 1979. Morphological stabilization of capsules of group B streptococci, types 1a, 1b, II, III, with specific antibody. J. Bacteriol. **138**:609-617.
23. **Maheswaran, S. K., and E. S. Thies.** 1979. Influence of encapsulation on phagocytosis of *Pasteurella multocida* by bovine neutrophils. Infect. Immun. **26**:76-81.
24. **Marsden, H. B., and W. A. Hyde.** 1971. Isolation of *Bacteroides corrodens* from infections in children. J. Clin. Pathol. **24**:117-119.
25. **Martin, H. H., H.-J. Preusser, and J. P. Verma.** 1968. Über die oberflächenstruktur von myxobakterien. II. Anionishe heteropolysaccharide als baustoffe der schleimhulle von *Cytophaga hutchinsonii* und *Sporocytophaga myxococcoides*. Arch. Mikrobiol. **62**:72-84.
26. **Newman, M. G., S. S. Socransky, E. D. Savitt, D. A. Propas, and A. Crawford.** 1976. Studies of the microbiology of periodontosis. J. Periodont. **47**:373-379.
27. **Onderdonk, A. B., D. L. Kasper, R. L. Cisneros, and R. L. Bartlett.** 1977. The capsular polysaccharide of *Bacteroides fragilis* as a virulence factor: comparison of the pathogenic potential of encapsulated and unencapsulated strains. J. Infect. Dis. **136**:82-89.
28. **Ottow, J. C. G.** 1975. Ecology, physiology, and genetics of fimbriae and pili. Annu. Rev. Microbiol. **29**:79-108.
29. **Pate, J. L., and E. J. Ordal.** 1967. The fine structure of *Chondrococcus columnaris*. III. The surface layers of *Chondrococcus columnaris*. J. Cell Biol. **35**:37-51.
30. **Reynolds, E. S.** 1963. The use of lead citrate at high pH as an electron-opaque stain for electron microscopy. J. Cell Biol. **17**:208-212.
31. **Savage, D. C.** 1972. Survival on mucosal epithelia, epithelial penetration, and growth in tissues of pathogenic bacteria. Symp. Soc. Gen. Microbiol. **22**:25-57.
32. **Schwarzmann, S., and J. R. Boring, III.** 1971. Antiphagocytic effect of slime from a mucoid strain of *Pseudomonas aeruginosa*. Infect. Immun. **3**:762-767.
33. **Scott, J. E., G. Quintarelli, and M. C. Dellovo.** 1960. The chemical and histochemical properties of alcian blue. I. The mechanism of alcian blue staining. Histochemistry **4**:73-85.

34. **Slots, J.** 1977. The predominant cultivable microflora of advanced periodontitis. Scand. J. Dent. Res. **85**:114–121.

35. **Slots, J., and E. Hausmann.** 1979. Longitudinal study of experimentally induced periodontal disease in *Macaca arctoides*: relationship between microflora and alveolar bone loss. Infect. Immun. **23**:260–269.

36. **Springer, E. L., and I. L. Roth.** 1973. The ultrastructure of the capsules of *Diplococcus pneumoniae* and *Klebsiella pneumoniae* stained with ruthenium red. J. Gen. Microbiol. **74**:21–31.

37. **Socransky, S. S.** 1977. Microbiology of periodontal disease-present status and future considerations. J. Periodont. **48**:497–504.

38. **Sutherland, I. W. (ed.).** 1977. Surface carbohydrates of the prokaryotic cell, p. 27–88. Academic Press, London.

39. **Tanner, A. C. R., C. Haffer, G. T. Bratthall, R. A. Visconti, and S. S. Socransky.** 1979. A study of the bacteria associated with advancing periodontitis in man. J. Clin. Periodontol. **6**:278–307.

40. **Thyberg, J., S. Lohmander, and U. Friberg.** 1973. Electron microscopic demonstration of proteoglycans in guinea pig epiphyseal cartilage. J. Ultrastruct. Res. **45**: 407–427.

41. **van Palenstein Helderman, W. H.** 1975. Total viable count and differential count of *Vibrio* (*Campylobacter*) *sputorum, Fusobacterium nucleatum, Selenomonas sputigena, Bacteroides ochraceus,* and *Veillonella* in the inflamed and noninflamed human gingival crevice. J. Periodont. Res. **10**:294–305.

42. **Wilkinson, B. J., P. K. Peterson, and P. G. Quie.** 1979. Cryptic peptidoglycan and the antiphagocytic effect of the *Staphylococcus aureus* capsule: model for the antiphagocytic effect of bacterial cell surface polymers. Infect. Immun. **23**:502–508.

43. **Woo, D. D. L., S. C. Holt, and E. R. Leadbetter.** 1979. Ultrastructure of *Bacteroides* species: *Bacteroides asaccharolyticus, Bacteroides fragilis, Bacteroides melaninogenicus* subspecies *melaninogenicus,* and *B. melaninogenicus* subspecies *intermedius.* J. Infect. Dis. **139**:534–546.